Assessing the impact of climate changes on the distribution of two corn diseases: corn stunt and corn reddening

José Carlos Barbosa Dos Santos, Rodrigo Soares Ramos, DAIANE DAS GRAÇAS Do CARMO, Marcelo Coutinho Picanco, Eliseu Pereira Guedes, Paulo Antônio Santana Junior, Renato Almeida Sarmento, NATÁLIAX De SOUZA RIBAS, George Correa Amaro & RICARDO SIQUEIRA Da SILVA

View supplementary material ⧉

Published online: 05 Aug 2025.

Submit your article to this journal ⧉

Article views: 11

View related articles ⧉

View Crossmark data ⧉

Taylor & Francis
Taylor & Francis Group

Check for updates

Epidemiology / Épidémiologie

Assessing the impact of climate changes on the distribution of two corn diseases: corn stunt and corn reddening

JOSÉ CARLOS BARBOSA DOS SANTOS [1], RODRIGO SOARES RAMOS[2],
DAIANE DAS GRAÇAS DO CARMO[2], MARCELO COUTINHO PICANCO[2,3], ELISEU PEREIRA GUEDES[2],
PAULO ANTÔNIO SANTANA JUNIOR[2], RENATO ALMEIDA SARMENTO[4], NATÁLIAX DE SOUZA RIBAS[1],
GEORGE CORREA AMARO[5] AND RICARDO SIQUEIRA DA SILVA[1]

[1]*Department of Agronomy, Universidade Federal dos Vales do Jequitinhonha e Mucuri (UFVJM), Diamantina, Brazil*
[2]*Department of Entomology, Universidade Federal de Viçosa, Viçosa, Brazil*
[3]*Department of Plant Science, Universidade Federal de Viçosa, Viçosa, Brazil*
[4]*Programa de Pós-graduação em Produção Vegetal, Universidade Federal do Tocantins, Gurupi-TO, Brazil*
[5]*Scientific Research, Embrapa Roraima, Boa Vista, Brazil*

Abstract: Corn stunt (CS) and corn reddening (CR) are considered the main phytosanitary problems of corn crops in the Neotropical region, caused by *Spiroplasma kunkelii* and *Candidatus* Phytoplasma ssp., respectively. Models that evaluate the potential geographic distribution of CS and CR are important to know which regions and areas are suitable for formulating appropriate policies and preventive measures. This study aimed to identify highly suitable areas and assess the impact of climate change on the distribution of CS and CR. To do this, we developed two spatial distribution models for CS and CR. We found 193 points of occurrence for CS and 158 points for CR. Considering its biology and ecology, we used R-based analysis version 4.4.0 'Puppy Cup' to predict potential global distribution of CS and CR using bioclimatic variables. We found that the most critical abiotic variables driving the global distribution of CS were: mean diurnal range, maximum temperature of the warmest month, and temperature seasonality. For the global distribution of CR, the most important variables were: isothermality, mean diurnal range, precipitation of the warmest quarter, and precipitation of the driest quarter. With regard to the validation of the forecast (2041–2060), the SSP2–4.5 models showed greater adaptability in the world's main corn-producing countries: the United States, China and Brazil. On the other hand, for SSP5–8.5, Maxent predicted that suitable CS and CR habitat will decrease by 2060 in the United States, China and Brazil. These countries showed a significant reduction in the occurrence of CS and CR. Our modelling results will provide helpful information to determine the spatial distribution of CS and CR and outline implications for monitoring through the risks of these diseases based on climatic conditions worldwide, especially in SSP2–4.5 senarios.

Keywords: Climate change, crop protection, MaxEnt, species distribution

Résumé: Le syndrome du nanisme du maïs (CS) et le rougeoiement du maïs (CR) sont considérés comme les principaux problèmes phytosanitaires des cultures de maïs dans la région néotropicale, causés respectivement par *Spiroplasma kunkelii* et *Candidatus Phytoplasma ssp*. Des modèles évaluant la distribution géographique potentielle de CS et CR sont essentiels pour identifier les régions propices et ainsi mettre en place des politiques et des mesures préventives adéquates. Cette étude avait pour objectif d'identifier les zones fortement appropriées et d'évaluer l'impact du changement climatique sur la répartition de CS et CR. Pour cela, deux modèles spatiaux de distribution ont été développés, l'un pour CS et l'autre pour CR. Nous avons identifié 193 points d'occurrence pour le syndrome du nanisme du maïs (CS) et 158 points pour le rougeoiement du maïs (CR). En tenant compte de leur biologie et écologie, nous avons utilisé R version 4.4.0, également connu sous le nom de « Puppy Cup », pour prédire la distribution géographique globale potentielle de CS et CR en utilisant des variables bioclimatiques. Notre analyse a révélé que les variables abiotiques les plus cruciales influençant la distribution mondiale du

syndrome du nanisme du maïs (CS) étaient : l'amplitude thermique diurne moyenne, la température maximale du mois le plus chaud, et la saisonnalité thermique. Pour la distribution mondiale du rougeoiement du maïs (CR), les variables bioclimatiques les plus déterminantes identifiées étaient l'isothermicité, l'amplitude thermique diurne moyenne, les précipitations durant le trimestre le plus chaud et celles du trimestre le plus sec. En regard de la validation des projections climatiques pour la période 2041–2060, les modèles fondés sur le scénario SSP2–4.5 (émissions modérées) montrent une meilleure adéquation dans les principaux pays producteurs de maïs, à savoir les États-Unis, la Chine et le Brésil. À l'inverse, sous le scénario plus sévère SSP5–8.5 (émissions élevées), les modèles MaxEnt prévoient une réduction des zones climatiquement favorables à la présence de CS et CR d'ici 2060 dans ces trois pays. Ces pays ont montré une réduction significative de l'occurrence du syndrome du nanisme du maïs (CS) et du rougeoiement du maïs (CR). Nos résultats de modélisation offrent des informations précieuses pour déterminer la distribution spatiale potentielle de CS et CR, et pour formuler des implications pour la surveillance des risques de ces maladies en fonction des conditions climatiques mondiales, en particulier dans les scénarios du type SSP2–4.5.

Mots-clés: changement climatique, distribution des espèces selon MaxEnts, protection des cultures

Introduction

Climate change is a long-term transformation in temperature and weather patterns (Ghanem 2024). These changes can be natural, due to changes in the Sun's activity or volcanic eruptions. Human activities have been the main driver of climate change, mainly due to the burning of fossil fuels such as coal, oil, and gas. Climate change can be divided into different types of scenarios. Climate scenarios are plausible descriptions of the risks of climate change and identify possible solutions with political measures. Among the types of scenarios, there are optimistic and pessimistic scenarios. The optimistic scenario (SSP126) describes that, by 2100, the planet's air temperature will increase by 2°C. The pessimistic scenario (SSP585) describes that, by 2100, the planet's air temperature will increase by 4°C to 5.5°C. Climate change exacerbates outbreak risks by changing the way pathogens evolve and interact with hosts. The range of pathogens can shift, leading to the increased spread of plant diseases into previously unaffected regions (Singh et al. 2023). The main factors that limit the growth and development of diseases and their vectors are temperature and rain (Elad and Pertot 2014; Ramos et al. 2018; Picanco et al. 2024). As a result, global warming will cause significant impacts on the distribution patterns and the physiological and ecological characteristics of organisms (Bellard et al. 2012; Elad and Pertot 2014). These alterations can adversely affect the productivity of food crops within agricultural systems (Wheeler and von Braun 2013; Crespo-Perez et al. 2015). Consequently, forecasting pest distribution under both current and future climatic conditions is crucial for making informed decisions and developing effective strategies to mitigate risks in agricultural systems (Crespo-Perez et al. 2015; Ramos et al. 2018; Santana et al. 2019; Aidoo et al. 2022).

Corn (*Zea mays* L.) holds a significant role as a staple food globally, with the highest consumption rate compared to other grain crops (FAO 2022). This crop is suitable for all growing seasons in almost all agro-climatic zones. Corn faces a series of threats and diseases throughout its phenological phases and is a host of 130 different pests and about 110 diseases caused by fungi, bacteria, and viruses worldwide. Control of diseases is essential to maintain reasonable production rates in this crop. Major corn diseases include corn stunt (CS; *Spiroplasma kunkelii*) and corn reddening (CR; *Candidatus Phytoplasma* ssp.) (Nault 1980; Oliveira and Frizzas 2022; Canale Nesi et al. 2023).

Corn stunt and corn reddening are diseases caused by microorganisms known as mollicutes, belonging to *Spiroplasma* (Entomoplasmatales: Spiroplasmataceae), and Phytoplasma (Acholeplasmatales: Acholeplasmataceae), respectively (Nault 1980). These microorganisms are transmitted exclusively by the leafhopper *Dalbulus maidis* (DeLong and Wolcott 1923) (Hemiptera: Cicadellidae) (Waquil et al. 1999; Oliveira and Frizzas 2022). Mollicutes invade systemically and multiply in the phloem tissues of the corn plant. Plants infected with these pathogens have shorter internodes, fewer roots, and produce fewer grains than healthy plants. Both CS and CR cause damage to grain production in corn-producing regions. For example, in one region in Brazil, the potential loss caused by stunting exceeded $16.5 million in losses for corn producers, with damage levels up to 100% (Virla et al. 2021; Neves et al. 2022; Oliveira and Frizzas 2022).

Ecological niche models are utilized to identify suitable areas or periods for a particular species (Elith and Leathwick 2009; Kumar et al. 2014; Nguyen and Leung 2022). Climate change can impact the way pathogens interact with their environment by affecting their growth and survival. Due to their quick reproductive rates, the ability to move easily, and sensitivity to temperature changes, pathogens are likely to be significantly impacted by even small shifts in climate, leading to rapid changes in their distribution and numbers (Raza

and Bebber 2022; Singh et al. 2023). The models can predict current locations suitable for pathogens and where they are not yet present and make predictions for the future under climate change (Hill et al. 2024). Ecological niche models are models that determine suitable areas or times for one or more species. These models can be divided into mechanistic models, which use the species climatic thresholds, e.g., Climex, and machine learning models, which are artificial intelligence tools that develop models capable of learning patterns from real data, e.g., MaxEnt (Kumar et al. 2014; Ramos et al. 2018; da Silva et al. 2020; Aidoo et al. 2022). However, to date, we have found very few papers with relation to the potential effects of climate change on the geographic distribution of CS and CR using ecological niche modelling. This study aimed to assess the impact of climate change on the distribution of CS and CR using correlative modelling.

Materials and methods

Species occurrence data

To identify the highly suitable areas and the effects of climate change on the distribution of CS and CR, we developed two spatial distribution models. The occurrence of corn stunt and corn reddening worldwide were downloaded from the Centre for Agriculture and Bioscience International (CABI: https://www.cabi.org), and the Global Biodiversity Information Facility (GBIF: https://www.gbif.org/). These data were complemented by published journal articles from Semantic Scholar (semanticscholar.org), Google Scholar (https://scholar.google.com.), and Web of Science (https://www.webofknowledge.com). To better represent the occurrence of the species worldwide, peer-reviewed articles in any year were considered for this study (Supplementary Tables S1 and S2). The keywords used were 'Corn Stunt + occurrence world', 'Corn reddening + occurrence world', 'CS in the corn/maize', 'Maize Bushy Stunt + occurences, Maize Bushy Stunt + maps', 'Corn Reddening in corn/maize', 'CR in corn/maize', 'Corn stunt disease' and 'CS in corn/maize'. A total of 193 and 158 records were found for CS and CR, respectively. For performing the analysis, we obtained the location (region with infected corn plants), latitude, longitude, disease type (CS or CR), and references (Supplementary Tables S1 and S2) where these diseases were reported in the data where we found their occurrence. Various procedures for cleaning occurrence data were adopted: (a) only records with a spatial resolution ≤1 km were retained for analysis; (b) occurrence records with a radius of 10 km around the centers of

capital cities and 5 km around the centers of countries, states, and provinces/municipalities were removed; (c) those with the same absolute longitude and latitude, a radius of 0.5 degrees around the GBIF headquarters, duplicate coordinates, and zero values were also removed; and (d) records located in water or that had not been associated with all the selected environmental variables were removed (Ramos et al. 2018; Santana et al. 2019; Aidoo et al. 2022; Wang et al. 2023).

Accounting for sampling bias is the biggest challenge faced by presence-only and presence-background species distribution models; no matter what type of model is chosen, the use of biased data will mask the true relationship between occurrences and predictor variables (Barber et al. 2022; Schartel and Cao 2024).

A filter in environmental space was applied to reduce sampling bias. As environmental filters are sensitive to bin size, four bin sizes were tested (4, 6, 8, and 10). For each of them, the spatial autocorrelation between the filtered records was calculated based on Moran's I and the number of filtered records. Next, the number of bins with the lowest quartile of Moran's I was selected and, of these, the one with the highest number of records (Velazco et al. 2022). A regular multidimensional grid was then created in the environmental space determined by the predictor variables. The cell size of this grid was defined by the number of bins selected to divide the range of variable values into interval classes (Varela et al. 2014; Castellanos et al. 2019). Then, a single occurrence was randomly selected within each grid cell.

Occurrence data was partitioned to assess the model's performance using spatial block cross-validation since this method allows the potential spatial autocorrelation between the model's training and test data to be controlled and its transferability to be assessed more adequately than other partitioning methods (Roberts et al. 2017; Valavi et al. 2019). Geographically structured data partitioning methods are especially useful for assessing the transferability of models to different regions or periods (Roberts et al. 2017; Santini et al. 2021). To select the best grid size (square blocks, similar to the checkboard scheme), 30 grids were generated with resolutions ranging from 0.5 (~56 km) to 5 degrees (~557 km), in four partitions, with a minimum of five occurrences per partition, using 80% of the presences for the autocorrelation test, and the one with: (a) the lowest spatial autocorrelation, by Moran's I; (b) the maximum environmental similarity, considering the Euclidean distance; and (c) the minimum difference in the number of records between training and test data, given by the standard deviation (Velazco et al. 2019).

Climate variables

In this study, a total of 19 bioclimatic parameters were utilized from the WorldClim version 2.1 (Fick and Hijmans 2017) dataset for both present-day and future scenarios, with an average spatial resolution of 2.5 minutes (~4.6 km at the equator), obtained with the {geodata} package version 0.6–2, to assess current climatic conditions, since they capture the annual variations and limiting factors that are known to influence the geographical distribution of species (Fick and Hijmans 2017). An elevation variable was added, the main source of which was the Shuttle Radar Topography Mission (SRTM), whose data are available between −60° and 60° latitude, supplemented with GTOP30 data for the higher latitudes (> 60°).

The selection of variables for the model was carried out through an iterative (data-driven) process based on adjustments and refinements of Maxent models during the modelling procedure, with the resulting variables being evaluated and complemented about their biological relevance.

Calibration area and background selection

The calibration area (CA) was considered to be equivalent to the species movement (M) region of the BAM diagram (Soberon and Peterson 2005; Phillips et al. 2006). The accessible area approach of the BAM framework was used, i.e., the CA was the theoretical target for defining the area accessible to the species. These areas depend on opportunities and restrictions to M, including areas where species could potentially be present (Soberon 2010; Barve et al. 2011; Mendes et al. 2020).

The size of the calibration area affects the model's performance metrics. The discrimination capacity of models (i.e., the ability to correctly distinguish presence and absence locations), for example, usually increases with the size of the calibration area (Anderson and Raza 2010; Barbet-Massin et al. 2012). This is mainly because larger areas tend to include more ecologically distant absences from presences, which are easier to distinguish (Lobo et al. 2008; VanDerwal et al. 2009). The model's ability to predict the probability of occurrence decreases with the size of the calibration area, since larger surfaces tend to include areas far from presence sites, which are not relevant for inferring the interaction between the species and the environment (Acevedo et al. 2012).

In some cases, different calibration areas, taking into account the characteristics of the occurrences, can be useful for exploring the different dynamics of a phenomenon, i.e., areas other than those delimited by the occurrences can be included (Elith et al. 2011). If the aim is to capture the potential distribution, the location data used to develop the model should ideally be extracted from the widest possible geographical and environmental range, provided that scientific criteria are used to define the extent and limits of the CA (Jarnevich et al. 2015; Sillero and Barbosa 2021).

Considering the method of biogeographic entities, the Köppen-Geiger climate zones with at least one occurrence record were used to delimit the CA as biotic regions, i.e., climatic and geographic units that share the environmental and historical adaptations of the species.

Presence-background-based distribution models, such as Maxent, estimate the relative probability of presence by comparing the sites of occurrence with a background (an environmental context), which consists of all the sites in the calibration area, i.e., sites where the species is present, as well as those without presence information, where its occurrence is unknown (Phillips et al. 2006; Elith et al. 2011; Aidoo et al. 2022).

The background sample should be chosen to reflect the environmental conditions that one is interested in contrasting with the occurrences, based on the spatial scale of the ecological issues of interest (Saupe et al. 2012). Thus, 10 000 points were selected, and randomly distributed throughout the calibration area, equally stratified to the presence points in each partition (Phillips and Dudík 2008; Barbet-Massin et al. 2012).

MaxEnt modeling

All procedures relating to data processing, model development and maps and graphs were carried out using the R environment, version 4.4.0 'Puppy Cup' (R Core Team, R 2023), in a fully automated framework, developed based on best practices and recommendations relating to species distribution modelling with Maxent (Sillero 2011; Merow et al. 2013; Santini et al. 2021). We used the following packages: {terra} version 1.7–78 and {sf} version 1.0–16, for the analysis and transformation of spatial data; {ENMeval} 2.0.4, for the selection of variables; {flexsdm} version 1.3.4, for all procedures, for all the species distribution modelling procedures, with features from {maxnet} version 0.1.4; {pROC} version 1.18.5, for graphs and ROC curve estimates; {tmap} version 3.3–4, to plot all the resulting maps; and {ggplot2} 3.5.1, to visualize the various results (Phillips et al. 2006; Wickham 2018).

The maximum entropy model (Maxent) was used through an inhomogeneous Poisson point process, since this method is among the most widely used to model

species distribution and has shown good performance compared to others (Phillips et al. 2006; Elith and Leathwick 2009; Elith et al. 2011; Valavi et al. 2019).

Presence-background models, such as Maxent, compare the environmental conditions available in the calibration area (defined by the background points) with the conditions used by the species as represented by their occurrences (Hirzel et al. 2006; Phillips et al. 2006). All the background locations where there is no record of the species occurring are considered to be available and unused conditions. In theory, these models can distinguish between suitable and unsuitable habitats, not directly providing the probability of finding the species in a given location, but rather an index of habitat suitability, i.e. the quality of the habitat for the survival and persistence of the species, which is specific to each modelling method (Sillero 2011; Acevedo et al. 2012). In general terms, the suitability of the habitat does not guarantee the presence of the species, nor does the unsuitability of the habitat guarantee its absence. To identify habitat suitability for a particular species, i.e. those sites that meet the environmental requirements of that species in the study area, presence-background or presence-only methods are preferable (Sillero and Barbosa 2021).

For Maxent models, the two main parameters to be adjusted are: (1) the regularization multiplier; and (2) the combinations of feature classes (Elith et al. 2011; Merow et al. 2013). The regularization multiplier (RM) determines the penalty associated with including variables or their transformations (features) in the model. Higher RM values impose a stronger penalty on model complexity and therefore result in simpler (flatter) forecasts (projections). The features determine the potential shape of the marginal response curves. A model that can only include linear classes is likely to be simpler than a model that can include all possible features.

Features are transformations of the original predictor variables used to build the model and can be linear, quadratic, threshold, hinge, product and categorical (Merow et al. 2013). Hinge features tend to make linear and threshold features redundant. One way to obtain a relatively smoother fitted model, similar to a generalized additive model, is to use only hinge features (Elith et al. 2011). Excluding product features creates an additive model that is easier to interpret, although less capable of representing complex interactions (Elith et al. 2011).

A first Maxent model (base model) was fitted (Maxent's default settings) using a data set with the coordinates of the presence and background points and the values of all the predictor variables at these points to evaluate and select the most important variables for the final model using 4-fold cross-validation.

A selection of data-driven variables was carried out: from the base model, iterate through all the variables, starting with the one with the greatest contribution (importance of the permutation); if the variable is correlated with other variables, considering the Spearman rank coefficient > |0.7|, a Jackknife test is carried out and, among the correlated variables, the one that decreases the model's performance the least when removed is removed, according to the True Skill Statistic (TSS) metric (Allouche et al. 2006; Brown and Anderson 2014). The process is repeated until the remaining variables are no longer correlated at the set level (Vignali et al. 2020).

Subsequently, to optimize the parsimony of the model, as many variables as possible were removed while preserving their performance, evaluated based on a single-exclusion Jackknife test and according to the TSS metric, considering a cut-off that keeps only those whose permutation percentage importance is greater than 3%. Reducing the number of predictors can limit overfitting and thus result in a model that generalizes better and therefore produces more accurate predictions for data not used during training (Vignali et al. 2020).

The final model was designed on a global scale. A probability of occurrence map was generated, given the local environmental conditions, with values between 0 and 1, with a resolution of 2.5 minutes. The result of the projection was divided into five fixed probability classes, dividing the probability of occurrence into: (a) inadequate (0–10%); (b) marginal (10–20%); (c) moderate (20–50%); (d) optimal (50–80%); and (e) high (80–100%). The area of each class is estimated and becomes the reference for assessing the effect of climate change.

The AUC, which is the area under the ROC (Receiver Operating Characteristic) curve, indicates the model's ability to distinguish between presences and absences (or pseudo-absences, or background) and, despite its limitations, is a statistic widely used to characterize the performance of SDMs (Allouche et al. 2006; Lobo et al. 2008; Schartel and Cao 2024). Graphs for evaluating the AUC and partial AUC, together with a presence only calibration graph, allow the evaluation of the models by the metrics to be complemented visually (Elith et al. 2011). While the AUC provides a general measure of performance, the partial AUC (pAUC) with a 10% threshold allows a more specific region of the ROC curve to be identified for decision-making.

Projections for future scenarios were made using downscaled global climate models (GCMs) from Coupled Model Intercomparison Projections (CMIP) 6, with data obtained from Worldclim 2.1. Three GCMs were used

(MRI-ESM2-0, MIROC6 and MPI-ESM1-2-HR) to calculate the average of three SSPs, which refer to the last iteration of scenarios used for the CMIP6 (SSP1–2.6: low greenhouse gas emissions (GHGs); SSP2–4.5: medium GHG emissions; and SSP5–8.5: high GHG emissions) and two time periods (2021–2040 and 2041–2060) because, despite using identical functions, the various GCMs differ greatly in their forecasts for the 21st century (von Storch et al. 2016; Yukimoto et al. 2019).

Results

Model performance and variable contribution

A total of 375 points referring to the distribution of CS and CR were identified, with the application of the environmental filter (10 bins, with Moran's I = 0.3555); these points were reduced to 193 points referring to CS (Fig. 1a) and another 158 to CR (Fig. 1b) for a total of 351 points. Both are centred mainly on South America, a region characterized by a tropical climate and of significant representation in the production of corn, the exclusive host of CS and CR. Corn reddening is present on four continents (America, Asia, Europe and Africa), which shows its great adaptability to climatic conditions and establishes a warning sign for corn-producing regions. For Brazilian states that produce the largest amount of corn, which are Mato Grosso (MT), Goias (GO) and Parana (PR), the model showed high suitability. Corn stunt is present only in the American continent, both in North and South America.
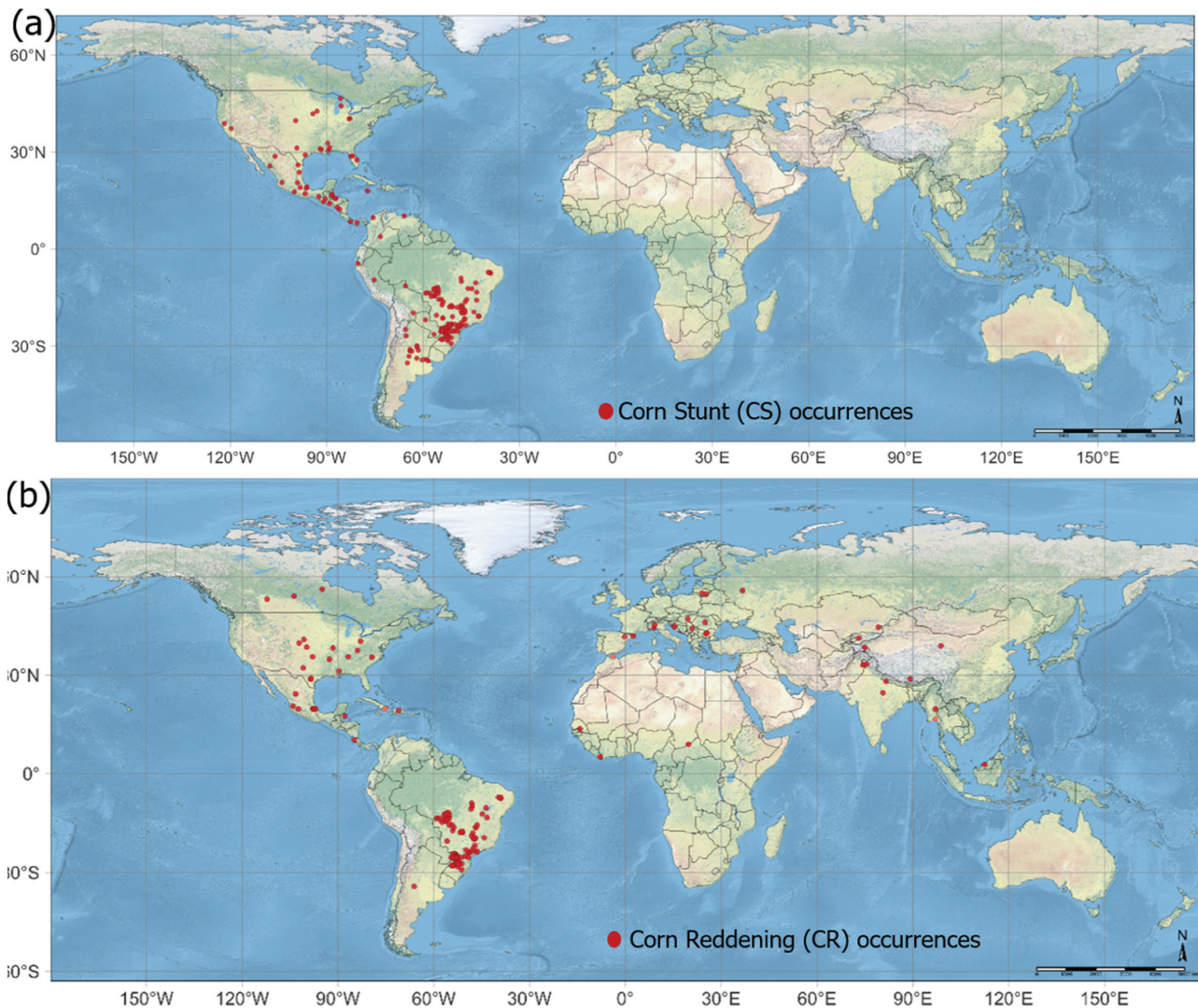
Fig. 1 Current global distribution for corn stunt (a) and corn reddening (b).

Figure 2, obtained with the {corrplot} package version 0.92, shows the covariates used, grouped according to the hierarchical cluster analysis, considering their correlation measured by the Spearman rank correlation coefficient (ρ), based on their values in the coordinates of occurrence.

The data-driven variable selection process, using Maxent itself with default parameters, resulted in seven variables for CS: 'Bio02', 'Bio04', 'Bio05', 'Bio15', 'Bio18', 'Bio19' and 'Elev' and seven variables for CR: 'Bio02', 'Bio03', 'Bio10', 'Bio15', 'Bio17', 'Bio18' and 'Bio19'. Descriptive statistics for these variables, considering their values in the coordinates of occurrence of CS and CR, are presented in Table 1, along with the others.

The fine adjustment resulted in a Maxent model with FC = QHP and RM = 0.5. Considering some of the most commonly used metrics (Table 2), such as the Boyce Index, which measures the sensitivity of the model and allowed it to identify 0.89% of the areas where the CS occurs and 0.93% of the area where the CR occurs, and TPR, which measures the sensitivity of the model and allowed it to identify 84.2% (CS) and 81.4 (CR) of the species' actual areas of occurrence, indicated whether the model tends to correctly predict suitable areas for the species. It can thus be inferred that the model developed was able to discriminate between the occurrences of the test data set and the background points adequately to identify the potential global geographical distribution of CS and CR.

Based on the pAUC, among the 10% of predictions with the highest probability of occurrence, 71.2 (CS) and 73.2% (CR) of unsuitable areas were correctly identified as such by the model (specificity), and 73.2% (CS) and 68.7% (CR) of the sites where the species is present were correctly identified as suitable (sensitivity), indicating that the model is reliable in identifying critical areas, with a slight inclination towards sensitivity, in agreement with the values observed in the metrics (Fig. 3).

Potential distribution under current climatic conditions

Considering the percentage importance of the permutation of variables in the final model (Fig. 4), of the seven variables used to fine-tune the Maxent model for CS and seven variables for CR, the four most important were, for CS: 'Bio2' (average diurnal variation), 'Bio5' (max temperature of warmest month) 'Bio4' (temperature seasonality) and elevation; and for CR, they were: 'Bio3' (isothermality), 'Bio2' (average diurnal variation), 'Bio18' (precipitation of warmest quarter) and 'Bio17' (precipitation of driest quarter), respectively.

Individual marginal response curves (partial dependence plots), which show the relationship between the probability of occurrence and each of the covariates, whereby the response is modelled for one variable while the others are kept constant at their mean along with frequency histograms and density curves of the values of the variables at the species' points of presence, are shown in Fig. 5 for the four variables with the highest percentage permutation importance in the final model. Inspection of the response curves shows that there are no bimodal responses, as expected.

The response curves show that the probability of CS occurrence is higher within localities with moderate mean diurnal range ('Bio2') > 11°C, with max temperature of the warmest month ('Bio5') varying between 24 and 37°C, and temperature seasonality ('Bio4') ranges varying between 30 and 80%. The response curves show that the probability of CR occurring is higher in locations with isothermality ranging between 60 and 80% ('Bio3'), with an average daytime temperature range between 13 and 17°C ('Bio2') and precipitation in the hottest quarter > 50 mm ('Bio18'). Additionally, the conditions identified suggest that CS can have a competitive advantage in temperate regions where the nights are cold and the days are warm, with relatively stable climates and moderate winter humidity, avoiding climatic extremes. Corn reddening occurs in areas mainly when there is a large variation within a month.

Figure 6 shows the potential geographical distribution of CS and CR for current climatic conditions. The highest related probabilities are centred mainly in South America, a region characterized by a tropical climate and with significant representation in the production of maize, the exclusive host of CS and CR. Corn redenning is present on four continents (America, Asia, Europe and Africa), which demonstrates its greater adaptability to climatic conditions and sets off a warning signal for maize-producing regions. For the Brazilian states that produce the most corn (MT, GO and PR), the model showed high suitability. On the other hand, CS is only present on the American continent, both in North and South America. The model showed 100% agreement with the occurrence records within the validation area by combining the estimated areas suitable for CS (Fig. 6a) and CR (Fig. 6b).

The specified probability classes (inadequate (0–10%), marginal (10–20%), moderate (20–50%), optimal (50–80%) and high (80–100%)) and the estimate of the corresponding areas, considering a resolution of 2.5 minutes, are presented in Fig. 7. Environments
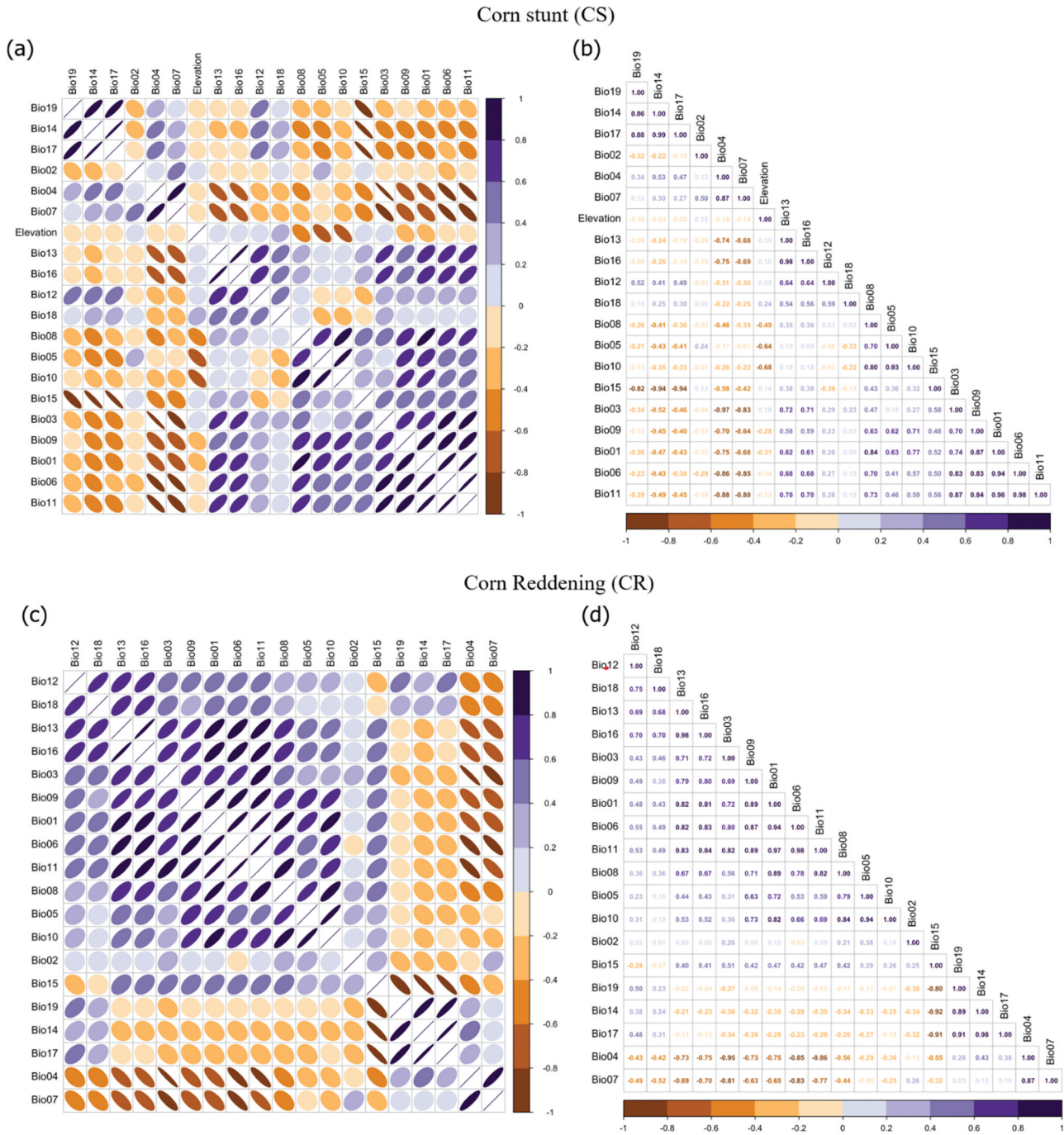
Fig. 2 Bioclimatic variable covariates and their correlation for corn stunt (CS; a, b) and corn reddening (CR; c, d). Correlation between bioclimatic variables: (a and c) the colour lilac with a slope to the right indicates a positive correlation, while orange with a slope to the left indicates a negative correlation. The intensity of the correlation coefficient increases as the shape changes from circle ($\rho = 0$) to ellipse ($\rho =$ intermediate) to line ($|\rho| = 1$); correlated variables were grouped by Ward's method (groups are more homogeneous internally, with the most heterogeneous among themselves) through hierarchical cluster analysis. Estimated values of the correlation coefficients between the variables, following the same colour pattern (b, d).

Table 1. Descriptive statistics of the covariates used in the models, considering their values in the coordinates of occurrence of corn stunt (CS) and corn reddening (CR). Variables that contributed to the model are in bold.

Variable	Variable Name	Minimum	Maximun	Median	Mean	SD
CS[a]						
Bio01	Annual Mean Temperature	4.82	27.84	20.10	20.55	3.82
Bio02	Mean Diurnal Range	8.65	18.31	12.48	12.42	**1.55**
Bio03	Isothermality	27.01	88.24	61.74	61.09	10.77
Bio04	Temperature Seasonality	27.64	1156.35	289.01	302.55	**209.77**
Bio05	Maximum Temperature of Warmest Month	23.13	37.39	30.51	30.63	**2.48**
Bio06	Minimum Temperature of Coldest Month	−13.99	22.37	9.13	9.44	6.13
Bio07	Temperature Annual Range	10.93	43.61	20.06	21.20	5.68
Bio08	Mean Temperature of Wettest Quarter	8.67	28.34	23.13	22.61	3.51
Bio09	Mean Temperature of Driest Quarter	−6.93	28.04	17.72	17.86	6.01
Bio10	Mean Temperature of Warmest Quarter	15.61	30.17	23.57	23.98	2.35
Bio11	Mean Temperature of Coldest Quarter	−7.55	27.30	16.13	16.66	6.11
Bio12	Annual Precipitation	299.00	3789.00	1578.00	1492.34	494.63
Bio13	Precipitation of Wettest Month	91.00	598.00	209.00	225.00	78.71
Bio14	Precipitation of Driest Month	0.00	145.00	31.00	46.33	42.02
Bio15	**Precipitation Seasonality**	**9.58**	**191.62**	**53.02**	**54.54**	**30.30**
Bio16	Precipitation of Wettest Quarter	211.00	1350.00	548.00	601.06	211.69
Bio17	Precipitation of Driest Quarter	0.00	508.00	126.00	169.53	146.18
Bio18	**Precipitation of Warmest Quarter**	**8.00**	**824.00**	**491.00**	**465.28**	**159.10**
Bio19	**Precipitation of Coldest Quarter**	**1.00**	**1024.00**	**161.00**	**218.70**	**187.19**
Elevation	**Elevation**	**3.00**	**2214.00**	**481.00**	**514.10**	**368.51**
CR[a]						
Bio01	Annual Mean Temperature	−4.15	27.24	19.10	17.91	6.45
Bio02	**Mean Diurnal Range**	**6.08**	**17.87**	**12.79**	**12.45**	**1.88**
Bio03	**Isothermality**	**21.46**	**89.69**	**60.14**	**56.82**	**14.59**
Bio04	Temperature Seasonality	40.42	1505.62	310.14	383.29	301.20
Bio05	Maximum Temperature of Warmest Month	13.86	42.25	29.62	29.30	4.30
Bio06	Minimum Temperature of Coldest Month	−29.77	22.50	7.94	5.68	9.46
Bio07	Temperature Annual Range	9.10	51.88	21.27	23.62	7.75
Bio08	Mean Temperature of Wettest Quarter	−3.48	28.97	22.29	20.46	5.18
Bio09	Mean Temperature of Driest Quarter	−20.70	29.86	16.21	14.67	9.34
Bio10	**Mean Temperature of Warmest Quarter**	**7.02**	**32.69**	**23.13**	**22.34**	**4.13**
Bio11	Mean Temperature of Coldest Quarter	−22.94	26.23	14.90	13.04	9.72
Bio12	Annual Precipitation	106.00	3502.00	1578.00	1380.25	566.91
Bio13	Precipitation of Wettest Month	19.00	460.00	209.00	208.03	87.80
Bio14	Precipitation of Driest Month	0.00	187.00	26.00	45.92	44.94
Bio15	**Precipitation Seasonality**	**9.58**	**141.44**	**48.23**	**53.25**	**31.38**
Bio16	Precipitation of Wettest Quarter	49.00	1266.00	539.00	552.63	241.67
Bio17	**Precipitation of Driest Quarter**	**0.00**	**620.00**	**88.00**	**167.13**	**154.46**
Bio18	**Precipitation of Warmest Quarter**	**48.00**	**832.00**	**455.00**	**421.45**	**188.88**
Bio19	**Precipitation of Coldest Quarter**	**3.00**	**1227.00**	**114.00**	**202.35**	**189.91**

[a]CS, corn stunt; CR, corn reddening.

with a high probability of occurrence of CS cover 1,570,399 km² and 2,176,929 km² for CR; and environments with an optimal probability cover 5,776,878 km² for CS and 3,296,249 km² for CR.

Figure 8 shows where there are conditions for the establishment of the species, by applying the Minimum Training Presence value, which represents the minimum environmental suitability that is still considered sufficient for the presence of the species (marginal conditions); and the 10th Percentile Training Presence, which considers only the top 90% of the presence points as suitable, ignoring the bottom 10%, reducing the inclusion of environments with marginal conditions.

Figure 9 shows the global projection of the presence/absence of CS and CR based on the application of a threshold that maximizes the sum of sensitivity and specificity (estimated at 0.3312), identifying the areas with the

Table 2. Metrics for evaluating the final Maxent model of corn stunt (CS) and corn reddening (CR).

Metric Names (CS)	Values	Metric Names (CR)	Values
True Positive Rate, Sensitivity or Recall (TPR)	0.84196	True Positive Rate, Sensitivity or Recall (TPR)	0.81394
True Negative Rate or Specificity (TNR)	0.82431	True Negative Rate or Specificity (TNR)	0.81164
True Skill Statistic (TSS)	0.66628	True Skill Statistic (TSS)	0.62558
Sorensen Index	0.15345	Sorensen Index	0.11056
Jaccard Index	0.08396	Jaccard Index	0.05870
F-measure on Presence-Background (FPB)	0.16792	F-measure on Presence-Background (FPB)	0.11741
Omission or False Negative Rate (OR)	0.15804	Omission or False Negative Rate (OR)	0.18606
Boyce Index	0.89161	Boyce Index	0.93303
Area Under ROC Curve (AUC)	0.88115	Area Under ROC Curve (AUC)	0.86926
Area Under Precision/Recall Curve (AUCPR)	0.21235	Area Under Precision/Recall Curve (AUCPR)	0.23340
Inverse Mean Absolute Error (IMAE)	0.87886	Inverse Mean Absolute Error (IMAE)	0.86945
False Positive Rate (FPR)	0.17569	False Positive Rate (FPR)	0.18836
Positive Predictive Value or Precision (PPV)	0.82736	Positive Predictive Value or Precision (PPV)	0.81208
Negative Predictive Value (NPV)	0.49470	Negative Predictive Value (NPV)	0.49929
Accuracy	0.83314	Accuracy	0.81279
F1 Score	0.83460	F1 Score	0.81301
Balanced Accuracy	0.83314	Balanced Accuracy	0.81279
Matthews Correlation Coefficient (MCC)	0.66638	Matthews Correlation Coefficient (MCC)	0.62559
Minimum Training Presence (MTP)	0.01052	Minimum Training Presence (MTP)	0.00028
10th Percentile Training Presence (10TP)	0.06402	10th Percentile Training Presence (10TP)	0.06555
Symmetric Extremal Dependence Index (SEDI)	0.81504	Symmetric Extremal Dependence Index (SEDI)	0.77982

CS, corn stunt; CR, corn reddening.

highest probability of the species occurring based on the conditions established by the selected climatic variables.

Potential distribution under future climate conditions

The models predict the suitable distribution areas of CS and CR on a global scale in the future (2041–2060) in two different scenarios (SSP2–4.5 and SSP5–8.5). In the SSP2–4.5 scenario (2041–2060), the MaxEnt model predicted that CS would have a highly suitable habitat on the American continent. Concerning the validation of the forecast (2041–2060), the models showed greater adaptability in the world's main corn-producing countries: the United States, China and Brazil. On the other hand, for SSP5–8.5, Maxent predicted that suitable CS and CR habitat will decrease by 2060 in the United States and China, Brazil. These countries showed a significant reduction in the occurrence of CS and CR. A reduction in the extent of suitable habitat was observed across the entire area of suitable habitat in the climate change scenarios (Fig. 10).

Discussion

This work is the first that has been undertaken to assess suitable areas for CS and CR and the impact of climate change on these diseases worldwide, currently and in the future using R-based analysis version 4.4.0 'Puppy Cup'.

The results were based on climatic requirements that combine the necessary environmental adequacy for CS and CR to survive in corn. Our model represented 100% of occurrence records within the validation area by combining the estimated suitable areas for point occurrences of CS and CR by modelling through MaxEnt in R-based analysis version 4.4.0 'Puppy Cup'. Our model highlights favourable and unfavourable regions for the distribution of CS and CR, highlighting the main factors limiting the climatic adequacy of the current time and future time.

Considering these assumptions, our model has a good fit with the current global distribution of CS and CR, including the areas used as validation, which provided data that were used to determine bioclimatic requirements. The consistency of the validation statistic for CS and CR projections demonstrates the models' reliability. Our results allow us to make reliable assumptions about suitable areas for the development of CS and CR around the world. In the proposed model, the bioclimatic variable related to annual precipitation played an important role in the projections of the spatial distribution of CS and CR.

Previous studies with polymerase chain reaction (PCR) tests indicated that CR was more tolerant to low temperatures than CS (Sabato et al. 2020). Nault (1980) found that the latent period of the CR pathogen, *Candidatus* Phytoplasma ssp., in its insect vector,
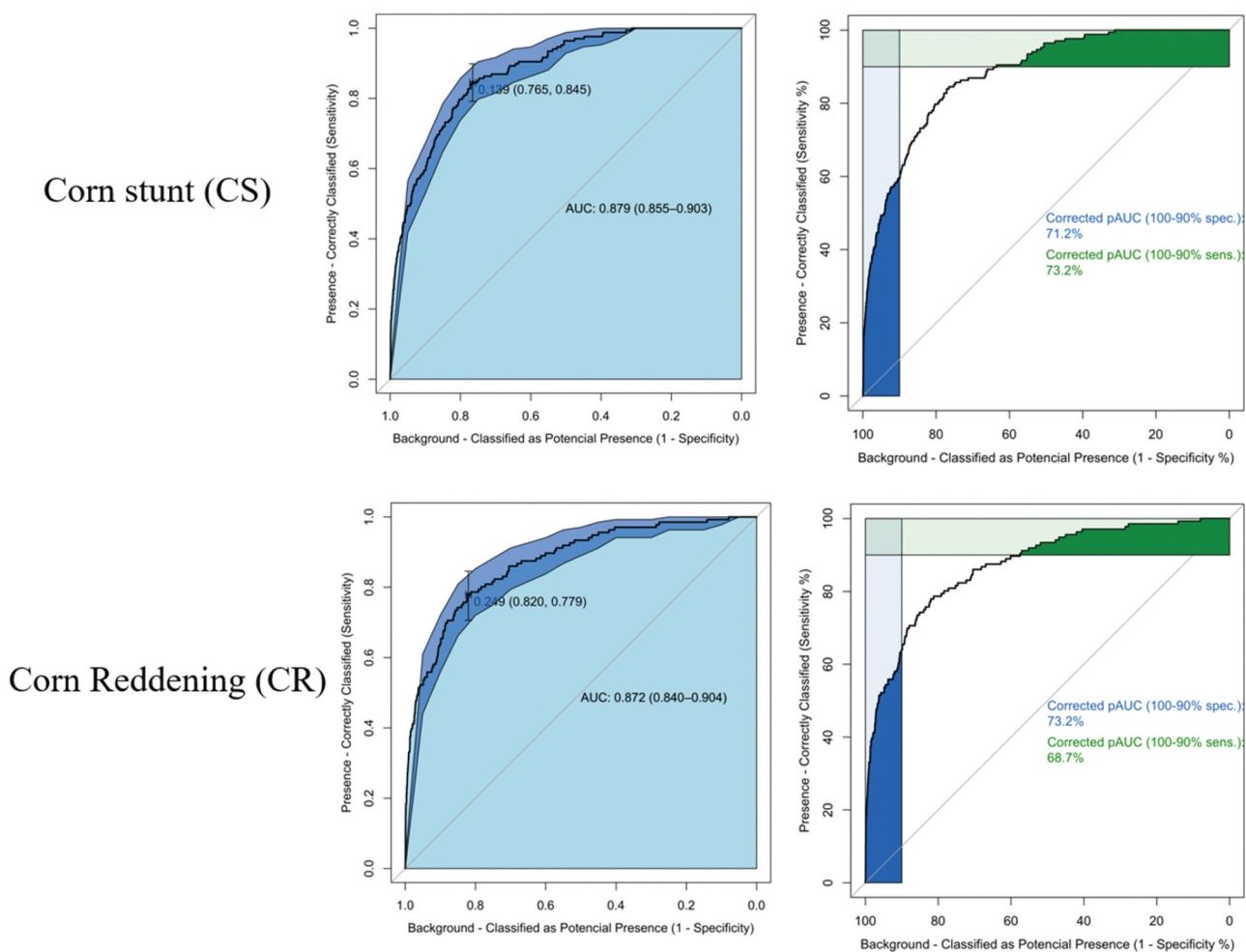
Fig. 3 Graphs of the area under the receiver operating characteristic (ROC) curve (AUC), partial AUC at 10% of the final Maxent model for corn stunt and corn reddening.
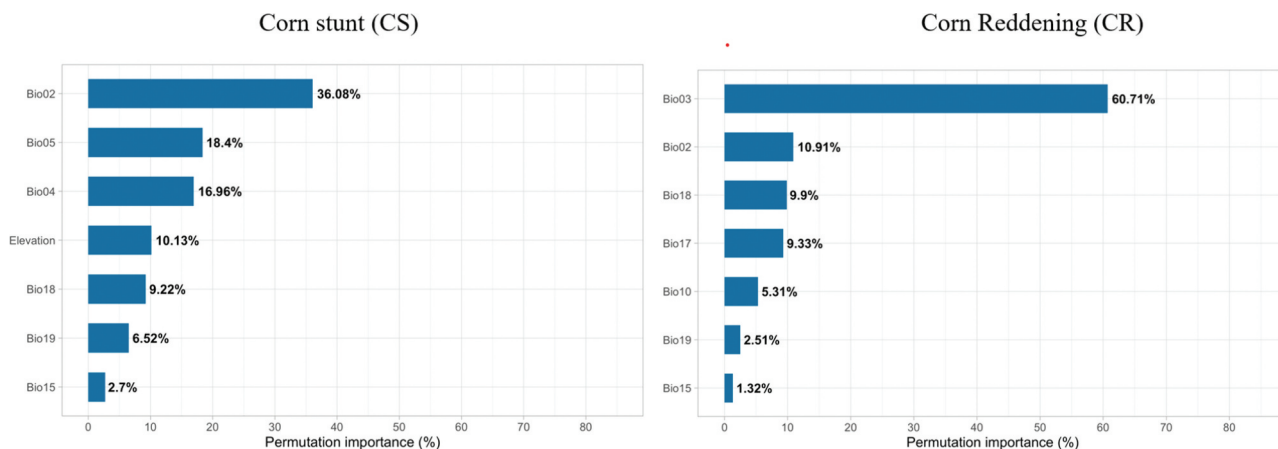

Fig. 4 Percentage importance of permutation of variables in the final Maxent model of corn stunt and corn reddening.
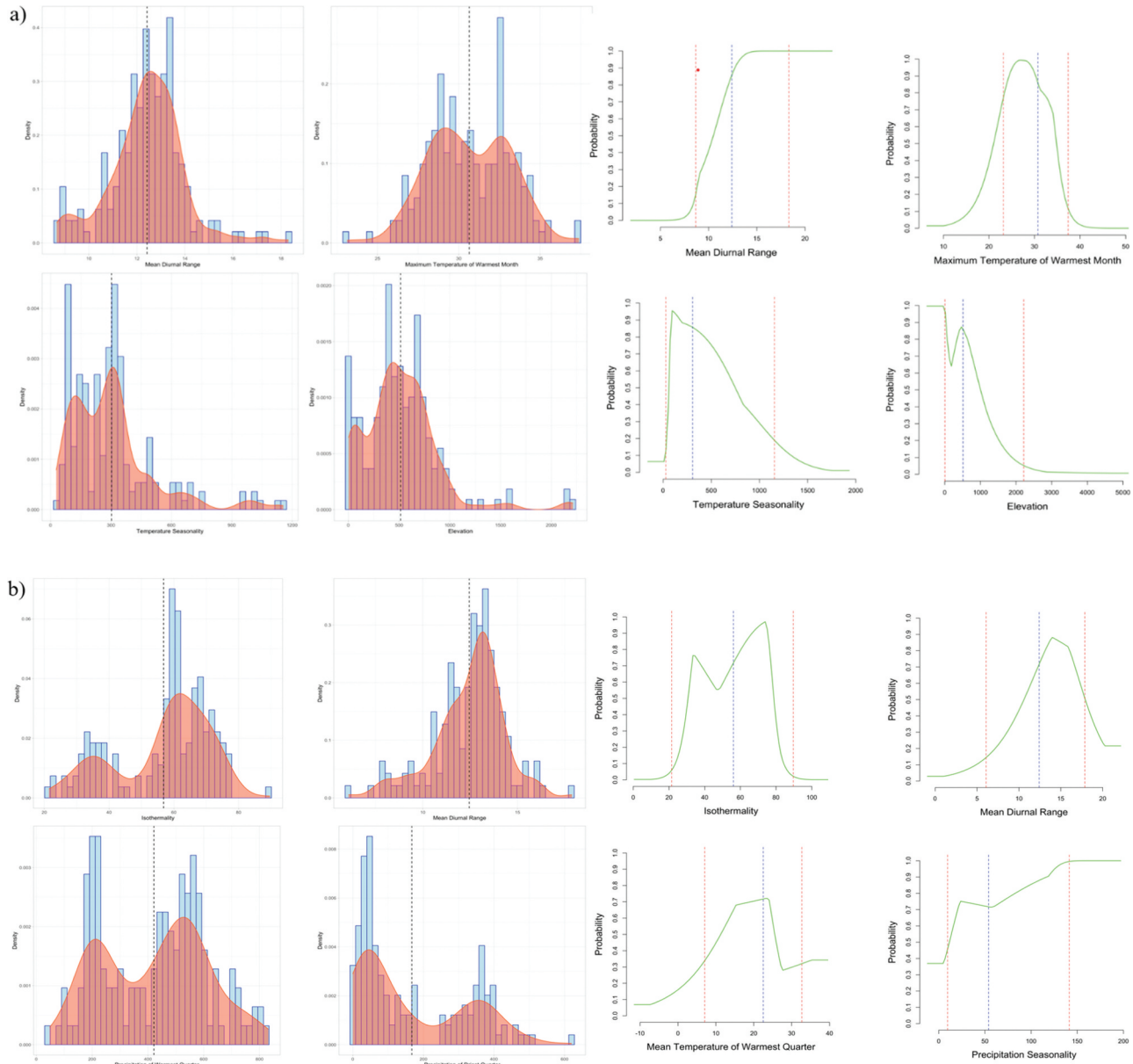
Fig. 5 Frequency histograms (in light blue) with density curves (considering only occurrences, in orange), and individual response curves (green lines) and and average values (dashed lines), from the final Maxent model of corn stunt (CS) (a) and corn reddening (CR) (b). Curves are presented for the important variables identified in the analyses presented earlier.

Daubulus maidis, and the transmission rate were lower in temperatures of 15°C and 30°C, and higher at temperatures of 20°C and 25°C. Therefore, in this work, we considered climate variables that are similar to other studies of CS and CR. Many factors can affect the distribution of diseases, such as the pathogen's ability to reach and develop at a potential site and to compete with other organisms occupying the same habitat (Raza and Bebber 2022; Singh et al.

2023). It is important to note that, in this study, we considered only the climatic suitability; and there are other factors that might limit the distribution of CS and CR in corn, such as geographic barriers, the characteristics of the insect vector, and natural enemies. In addition, spatial distribution studies have some uncertainties and, in general, there is consistency among the climate change projections of the different models. However, the magnitude of climate
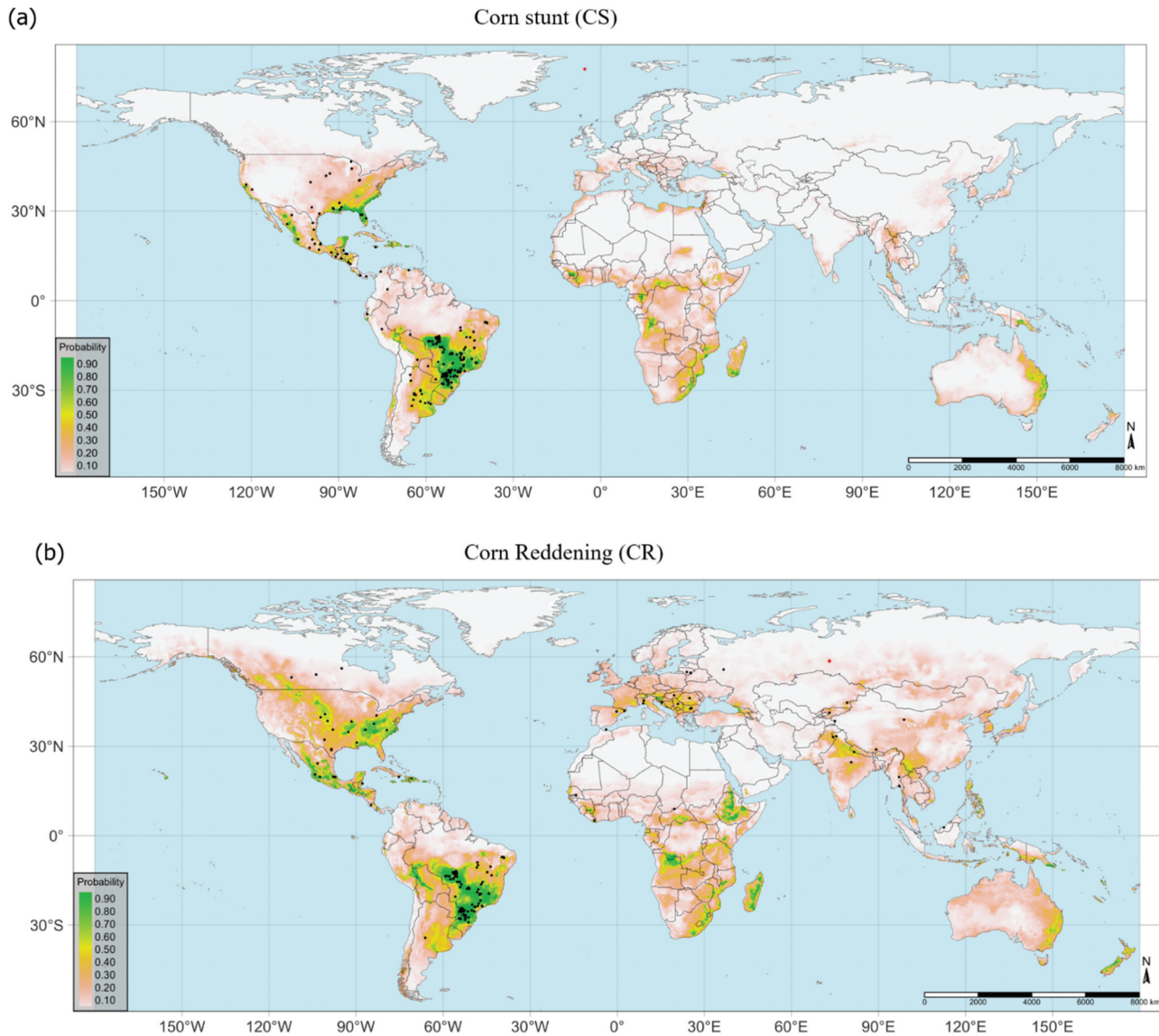
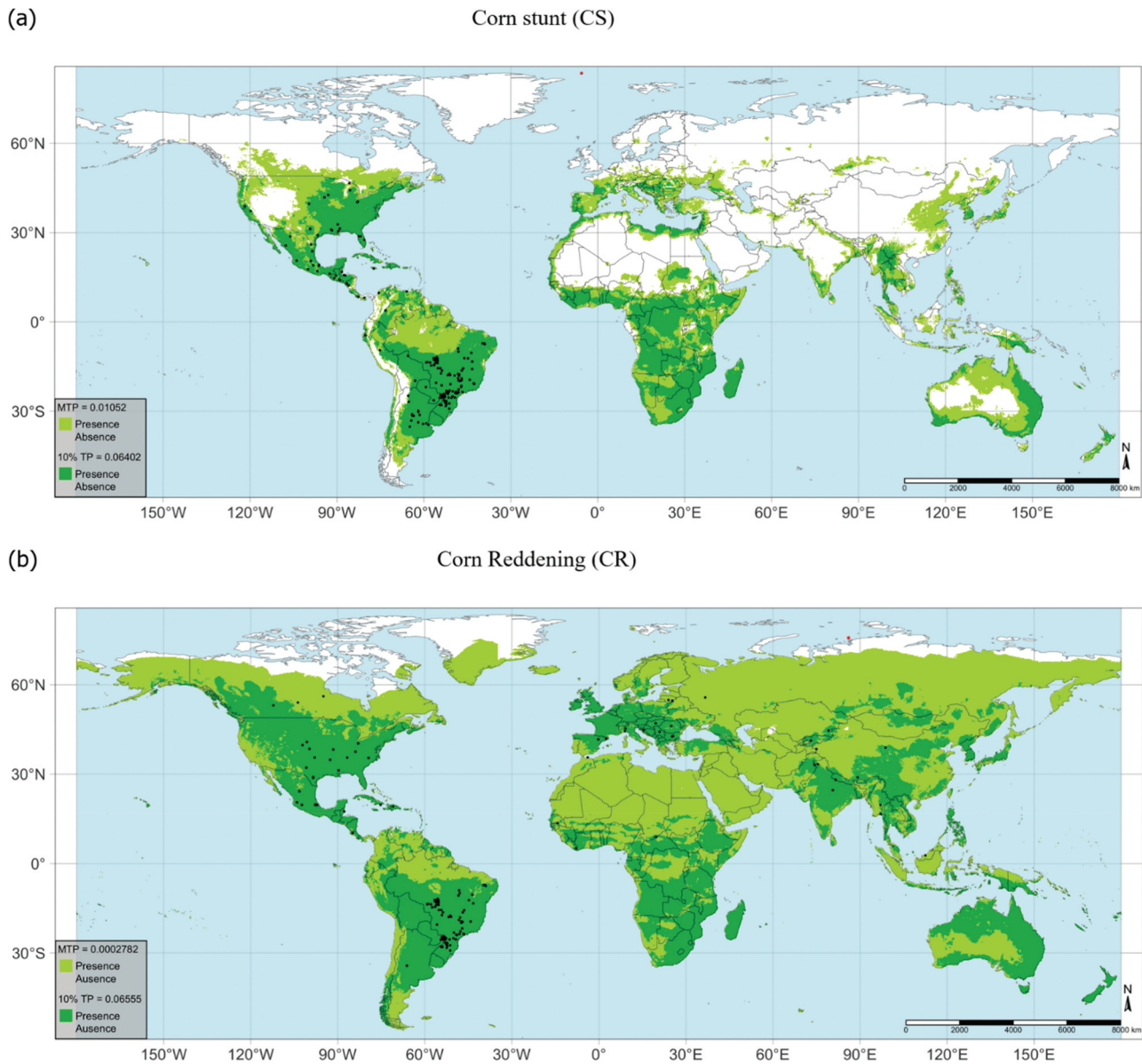**Fig. 6** Potential geographical distribution of corn stunt (CS) and corn reddening (CR) under current climatic conditions and points of confirmed occurrence of CS (a) and CR (b).

change strongly depends on the mitigation policies that may be applied in the future (IPCC 2020). The model's parameterization has to be performed in order to obtain results that are consistent. Therefore, the modler's knowledge and experience about the species are essential.

It is important to note that, in this study, we considered the climatic suitability for CS and CR. Pfordt and Paulus (2025) noted that accurate and early diagnosis of maize diseases is crucial for effective disease management, preventing infection and spread. Pozebon et al. (2022) pointed out that monitoring the incidence and severity of CS and CR in corn-producing regions, and relating this information to climatic data and characteristics, seems to be an important tool for determining the behaviour of these diseases over time. It is also useful for evaluating the effectiveness of adopting management measures at a regional level and allocating resources and prevention measures to the most problematic production areas.

(a)

Corn stunt (CS)

(b)
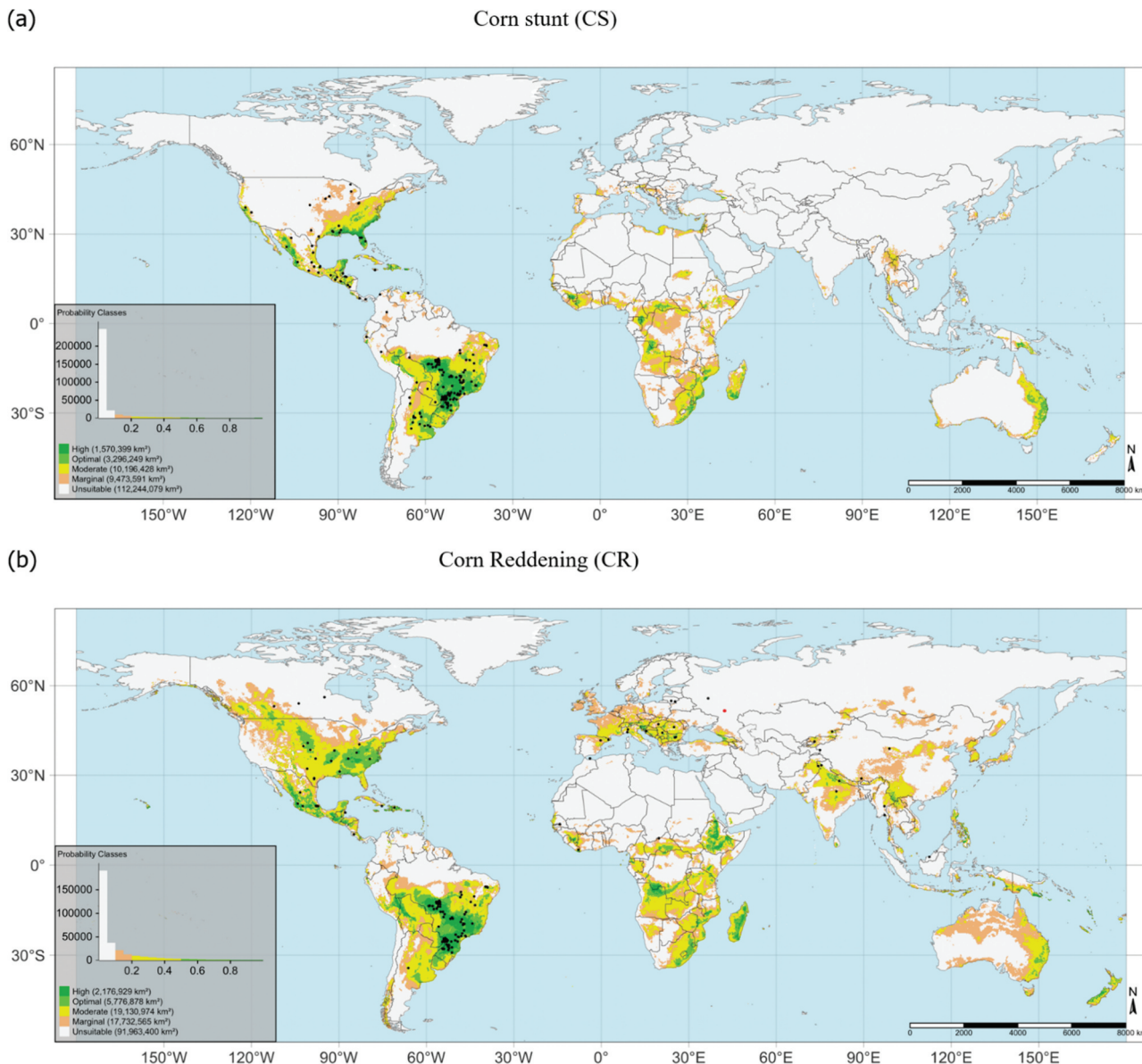
Corn Reddening (CR)

Fig. 7 Probability classes for the potential geographical distribution of corn stunt (a) and corn reddening (b) under current climatic conditions and estimates of areas (based on 30-second resolution) and points of confirmed occurrence of the species.

Currently, the digital transformation of agriculture is enabling the collection of vast amounts of georeferenced information about growing conditions within the field and facilitating the automated implementation of spatially varying input applications. This has the potential to increase production efficiency, reduce over-application of inputs, lower input waste and pollution and improve farm profitability with cost-effective adoption of digital technologies (Khanna 2021). Corn producers' use of technological tools is gaining more

and more prominence in the agricultural context. The results of our climate model can be helpful for the development of software that will facilitate the phyto-sanitary management of CS and CR occurrence in cornfields. Understanding the relationship between climate and disease is essential for developing software to facilitate phytosanitary management (Liu et al. 2015; Singh et al. 2023; Tonle et al. 2024).

The species distribution maps are of great importance for obtaining new information that can help improve a country's

Fig. 8 Potential geographical distribution of corn stunt (a) and corn reddening (b) considering the application of the threshold with minimum suitability for the species (marginal probability of occurrence) and the threshold that allows the identification of the most suitable areas (highest probability of occurrence, 10th Percentile Training presence) and points of confirmed occurrence of the species.

phytosanitary regulations and creating a strategic plan to avoid the dissemination of CS and CR. This study identified the most likely locations for the occurrence of both species and precisely determined the relationship between the environmental preferences of each species and the probability of CS and CR occurrence. These areas corresponded to areas in South America, Africa and small areas in the south of the United States, China and Brazil. Another important point is that regions of the world such as southeastern Australia and the African continent (Mamibia, Botswana, southeastern

South Africa, Madagascar, Mozambique and Tanzania) are regions where CS and CR have not yet occurred, but which are climatically suitable for the introduction of these diseases.

Comparing data from this work with data from CS and CR freely available online on the website of the Brazilian Ministry of Agriculture, Livestock and Supply (https://www.gov.br/agricultura/en-br/assuntos/sanidade-animal-e-vegetable/vegetable-health/corn-stunts), it is evident that our model p finds similar data,

(a)

Corn stunt (CS)

(b)
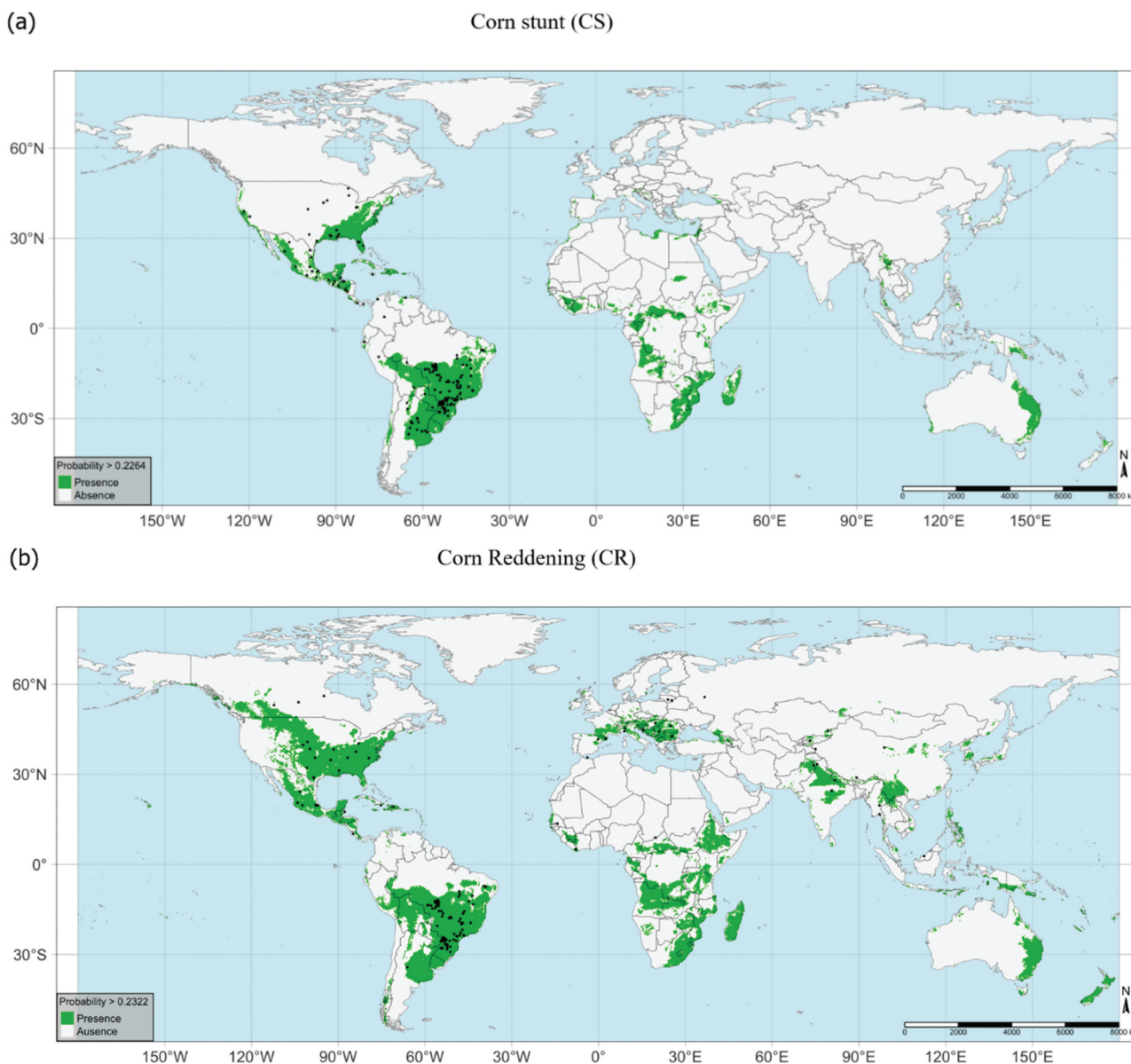
Corn Reddening (CR)

Fig. 9 Points of confirmed occurrence of the species and potential geographical distribution of corn stunt (CS) and corn reddening (CR) and considering the application of the threshold that maximizes the sum of sensitivity and specificity for (a) CS, maxSSS = 0.2264 and (b) CR, maxSSS = 0.2322.

since the CS and CR occurrence locations are exactly the same. In other research, Luedeling et al. (2011) reported the important effects of temperature on insect pests, and their results clearly indicate that generation numbers are going to rise for most pests, also using distribution maps. In addition, development and fitness of insect vector *D. maidis* vary with constant and threshold temperature, which may represent useful information for studies aiming to predict its potential distribution (Van Nieuwenhove et al. 2016).

This work considered climate variables in the current time period and 2041–2060 to determine suitability for CS and CR using MaxEnt model R-based analysis version 4.4.0 'Puppy Cup'. Thus, further studies considering other variables are necessary, such as the presence of other host species, seed treatments and resistant cultivars, among others. Suitability maps are important tools for pest risk analysis. These maps can support monitoring programs in countries where the species already occurs and determine guidelines and
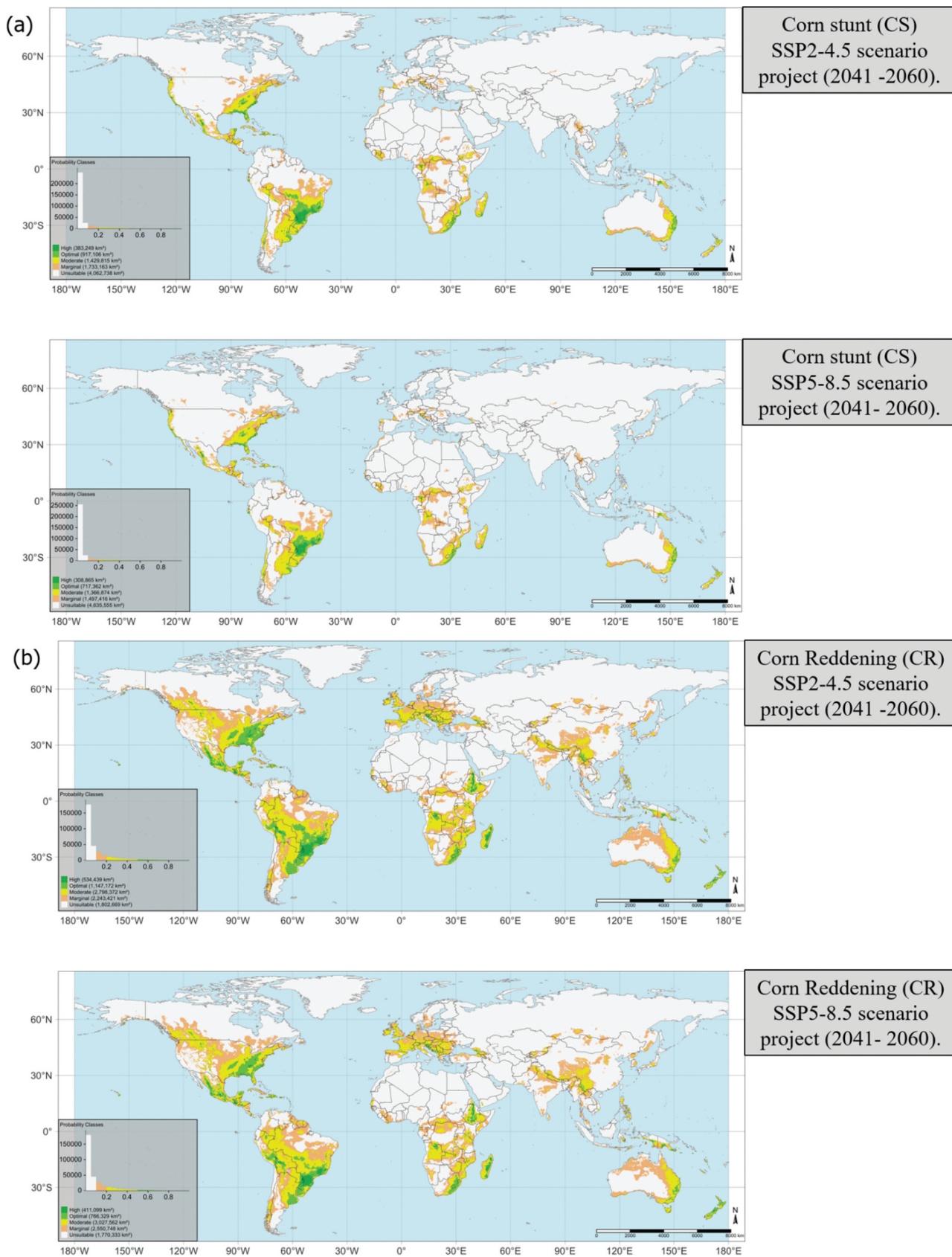
Fig. 10 Potential geographical distribution for corn stunt (a) and corn reddening (b), considering the average of different climate scenarios, expressed by continuous probability (0 to 1) and by defined probability classes (2.5-minute resolution).

measures to prevent the risk of invasion of CS and CR in other regions. These maps are also important tools for pest risk analysis, quarantine strategies and to support phytosanitary actions. These results can help develop strategies to suit CS and CR and support future research and supporting biosafety practices.

Conclusion

We assessed the impact of climate change on the distribution of two corn diseases: corn stunt and corn reddening. Locations with moderate mean diurnal range ('Bio2'), > 11°C, with the maximum temperature of warmest month ('Bio5') varying between 24 and 37°C, and temperature seasonality ('Bio4') varying between 100 and 750 mm, are climatically suitable for CS. The probability of CR occurring is higher in locations with isothermality ranging between 60 and 80% ('Bio3'), with the average daytime range varying between 13 and 17°C ('Bio2') and precipitation in the hottest quarter > 50 mm ('Bio18'). For Brazilian states, for example, that produce the biggest amount of corn (MT, GO, and PR) the model showed high suitability to both diseases in current time and future. There will be an increase in areas in the world with high ecoclimatic suitability for the disease, especially in 2070 and in climate change scenario SSP2–4.5. The results presented in this study show that, for future projections (2070), the American continent has greater climatic aptitude for CS, whereas for the African continent, the aptitude was smaller. Our models indicate that areas with a suitable climate for CS and CR occurrence will likely increase in corn-producing countries on the American continent and Western Europe. In contrast, corn-producing countries in Asia may have a reduced risk of CS and CR occurrence due to incompatible climate suitability.

Acknowledgments

Funding

Disclosure statement

No potential conflict of interest was reported by the authors.

Author contribution statement

JCBS, RSR, MCP, EPG, PASJ, RAS and RSS conceived and designed research. JCBS, PCL, RSR, PASJ, DGC, NSR, GCA and RSS acquired data. JCBS, RSR and GCA analyzed the data. All authors read the final manuscript.

Data availability statement

Data from the current study are available from the corresponding author upon reasonable request.

Ethical approval

This article does not contain any studies with human participants or animals performed by any of the authors.

Supplementary material

Supplemental data for this article can be accessed online at https://doi.org/10.1080/07060661.2025.2533964.

ORCID

José Carlos Barbosa Dos Santos http://orcid.org/0000-0001-8907-2753

References

Acevedo P, Jiménez-Valverde A, Lobo JM, Real R. 2012. Delimiting the geographical background in species distribution modelling. J Biogeogr. 39(8):1383–1390. doi: 10.1111/j.1365-2699.2012.02713.x.

Aidoo OF, Souza PGC, da Silva RS, Santana PA, Picanco MC, Kyerematen R, Sètamou M, Ekesi S, Borgemeister C, da Silva RS. 2022. Climate-induced range shifts of invasive species (*Diaphorina citri* Kuwayama). Pest Manag Sci. 78(6):2534–2549. doi: 10.1002/ps.6886.

Allouche O, Tsoar A, Kadmon R. 2006. Assessing the accuracy of species distribution models: prevalence, kappa and the true skill statistic

(TSS). J Appl Ecol. 43(6):1223–1232. doi: 10.1111/j.1365-2664.2006. 01214.x.

Anderson RP, Raza A. 2010. The effect of the extent of the study region on GIS models of species geographic distributions and estimates of niche evolution: preliminary tests with montane rodents (genus *Nephelomys*) in Venezuela. J Biogeogr. 37(7):1378–1393. doi: 10. 1111/j.1365-2699.2010.02290.x.

Barber RA, Ball SG, Morris RKA, Gilbert F, Leroy B. 2022. Target-group backgrounds prove effective at correcting sampling bias in Maxent models. Divers Distrib. 28(1):128–141. doi: 10.1111/ddi.13442.

Barbet-Massin M, Jiguet F, Albert CH, Thuiller W. 2012. Selecting pseudo-absences for species distribution models: how, where and how many? Methods Ecol Evol. 3(2):327–338. doi: 10.1111/j.2041-210X. 2011.00172.x.

Barve N, Barve V, Jiménez-Valverde A, Lira-Noriega A, Maher SP, Peterson AT, Soberón J, Villalobos F. 2011. The crucial role of the accessible area in ecological niche modeling and species distribution modeling. Ecol Modell. 222(11):1810–1819. doi: 10.1016/j.ecolmodel. 2011.02.011.

Bellard C, Bertelsmeier C, Leadley P, Thuiller W, Courchamp F. 2012. Impacts of climate change on the future of biodiversity. Ecol Lett. 15(4):365–377. doi: 10.1111/j.1461-0248.2011.01736.x.

Brown JL, Anderson B. 2014. SDMtoolbox: a python-based GIS toolkit for landscape genetic, biogeographic and species distribution model analyses. Methods Ecol Evol. 5(7):694–700. doi: 10.1111/2041-210X. 12200.

Canale Nesi CN, Castilhos RV, Castilhos RV. 2023. Abundance of *dalbulus maidis* and impact of maize rayado fino disease on different genotypes in field conditions in Santa Catarina, Brazil. Trop Plant Pathol. 48(6):675–684. doi: 10.1007/s40858-023-00609-1.

Castellanos AA, Huntley JW, Voelker G, Lawing AM, McCrea R. 2019. Environmental filtering improves ecological niche models across multiple scales. Methods Ecol Evol. 10(4):481–492. doi: 10.1111/2041-210X.13142.

Crespo-Perez V, Régnière J, Chuine I, Rebaudo F, Dangles O. 2015. Changes in the distribution of multispecies pest assemblages affect levels of crop damage in warming tropical Andes. Glob Chang Biol. 21(1):82–96. doi: 10.1111/gcb.12656.

da Silva RS, Fidelis EG, Amaro G, Ramos RS, Junior PAS, Picanco MC. 2020. Climate-based seasonal dynamics of the invasive red palm mite *Raoiella indica*. Pest Manag Sci. 76(11):3849–3856. doi: 10.1002/ps.5936.

DeLong DM, Wolcott GN. 1923. A new genus and species of fulgoridae (Homoptera) from the western hemisphere. J Appl Psychol. 31 (2):143–146.

Elad Y, Pertot I. 2014. Climate change impacts on plant pathogens and plant diseases. J Crop Improv. 28(1):99–139. doi: 10.1080/15427528. 2014.865412.

Elith J, Leathwick JR. 2009. Species distribution models: ecological explanation and prediction across space and time. Annu Rev Ecol Evol Syst. 40(1):677–697. doi: 10.1146/annurev.ecolsys.110308.120159.

Elith J, Phillips SJ, Hastie T, Dudík M, Chee YE, Yates CJ. 2011. A statistical explanation of MaxEnt for ecologists. Divers Distrib. 17 (1):43–57. doi: 10.1111/j.1472-4642.2010.00725.x.

FAO. 2022. Food and Agriculture organization of the United Nations. Crop livest prod 2022. [accessed 2024 Jan 4]. https://www.fao.org/fao stat/en/#data/QCL.

Fick SE, Hijmans RJ. 2017. WorldClim 2: new 1-km spatial resolution climate surfaces for global land areas. Int J Climatol. 37(12):4302–4315. doi: 10.1002/joc.5086.

Ghanem KZ. 2024. Climate changes and sustainability. Open J Ecol. 14 (1):17–53. doi: 10.4236/oje.2024.141002.

Hill JL, Grisnik M, Hanscom RJ, Sukumaran J, Higham TE, Clark RW. 2024. The past, present, and future of predator–prey interactions in a warming world: using species distribution modeling to forecast ectotherm–endotherm niche overlap. Ecol Evol. 14(3):1–21. doi: 10.1002/ece3.11067.

Hirzel AH, Le Lay G, Helfer V, Randin C, Guisan A. 2006. Evaluating the ability of habitat suitability models to predict species presences. Ecol Modell. 199(2):142–152. doi: 10.1016/j.ecolmodel. 2006.05.017.

IPCC. 2020. Intergovernmental panel on climate change. IPCC fourth assessment report. Climate change: synthesis Report. Geneva, Switzerland: Intergovernmental Panel on Climate Change.

Jarnevich CS, Stohlgren TJ, Kumar S, Morisette JT, Holcombe TR. 2015. Caveats for correlative species distribution modeling. Ecol Inf. 29 (P1):6–15. doi: 10.1016/j.ecoinf.2015.06.007.

Khanna M. 2021. Digital transformation of the agricultural sector: pathways, drivers and policy implications. Appl Econ Perspect Policy. 43 (4):1221–1242. doi: 10.1002/aepp.13103.

Kumar S, Neven LG, Yee WL. 2014. Evaluating correlative and mechanistic niche models for assessing the risk of pest establishment. Ecosphere. 5(7):1–23. doi: 10.1890/ES14-00050.1.

Liu Y, Hu J, Snell-Feikema I, Ms V, Lamsal A, Wimberly MC. 2015. Software to facilitate remote sensing data access for disease early warning systems. Environ Model Softw. 74:247–257. doi: 10.1016/j. envsoft.2015.07.006.

Lobo JM, Jiménez-Valverde A, Real R. 2008. AUC: a misleading measure of the performance of predictive distribution models. Glob Ecol Biogeogr. 17(2):145–151. doi: 10.1111/j.1466-8238.2007.00358.x.

Luedeling E, Steinmann KP, Zhang M, Brown PH, Grant J, Girvetz EH. 2011. Climate change effects on walnut pests in California. Global Change Biol. 17(1):228–238. doi: 10.1111/j.1365-2486.2010.02227.x.

Mendes P, Velazco SJE, de Andrade AFA, De Marco P, Andrade AFAD. 2020. Dealing with overprediction in species distribution models: how adding distance constraints can improve model accuracy. Ecol Modell. 431(June):109180. doi: 10.1016/j.ecolmodel. 2020.109180.

Merow C, Smith MJ, Silander JA. 2013. A practical guide to MaxEnt for modeling species' distributions: what it does, and why inputs and settings matter. Ecography (Cop). 36(10):1058–1069. doi: 10.1111/j. 1600-0587.2013.07872.x.

Nault LR. 1980. Maize Bushy stunt and corn stunt: a comparison of disease symptoms, pathogen host ranges, and vectors. Phytopathology. 70(7):659. http://www.apsnet.org/publications/phytopathology/backis sues/Documents/1980Abstracts/Phyto70_659.htm.

Neves TNC, Foresti J, Silva PR, Alves E, Rocha R, Oliveira C, Picanco MC, Pereira EJG. 2022. Insecticide seed treatment against corn leafhopper: helping protect grain yield in critical plant growth stages. Pest Manag Sci. 78(4):1482–1491. doi: 10.1002/ps.6766.

Nguyen D, Leung B. 2022. How well do species distribution models predict occurrences in exotic ranges? Glob Ecol Biogeogr. 31 (6):1051–1065. doi: 10.1111/geb.13482.

Oliveira C, Frizzas MR. 2022. Eight decades of *Dalbulus maidis* (DeLong and Wolcott) (Hemiptera, Cicadellidae) in Brazil: what we know and what we need to know. Neotrop Entomol. 51(1):1–17. doi: 10.1007/s13744-021-00932-9.

Pfordt A, Paulus S. 2025. A review on detection and differentiation of maize diseases and pests by imaging sensors. J Plant Dis Prot. 132 (1):1–21. doi: 10.1007/s41348-024-01019-4.

Phillips SJ, Anderson RP, Schapire RE. 2006. Maximum entropy modeling of species geographic distributions. Ecol Modell. 190(3–-4):231–259. doi: 10.1016/j.ecolmodel.2005.03.026.

Phillips SJ, Dudík M. 2008. Modeling of species distributions with Maxent: new extensions and a comprehensive evaluation. Ecography (Cop). 31(2):161–175. doi: 10.1111/j.0906-7590.2008. 5203.x.

Picanco MM, Guedes RNC, da Silva RS, Galvão C, Souza PGC, Barreto AB, Picanco MC, Lopes PHQ, Picanço MC. 2024 Dec. Unveiling the overlooked: current and future distribution dynamics of kissing bugs and palm species linked to oral chagas disease transmission. Acta Tropica. 258:107367. doi: 10.1016/j.actatropica.2024.107367.

Pozebon H, Stürmer GR, Arnemann JA, Rashed A. 2022. Corn stunt pathosystem and its leafhopper vector in Brazil. J Econ Entomol. 115 (6):1817–1833. doi: 10.1093/jee/toac147.

R Core Team, R. 2023. R: a language and environment for statistical computing 171–203. Vienna, Austria: R found. for stat. comp.

Ramos RS, Kumar L, Shabani F, Picanco MC, Yue B-S. 2018. Mapping global risk levels of *Bemisia tabaci* in areas of suitability for open field tomato cultivation under current and future climates. PLOS ONE. 13(6):1–20. doi: 10.1371/journal.pone.0198925.

Raza MM, Bebber DP. 2022. Climate change and plant pathogens. Curr Opin Microbiol. 70:102233. doi: 10.1016/j.mib.2022.102233.

Roberts DR, Bahn V, Ciuti S, Boyce MS, Elith J, Guillera-Arroita G, Hauenstein S, Lahoz-Monfort JJ, Schröder B, Thuiller W, et al. 2017. Cross-validation strategies for data with temporal, spatial, hierarchical, or phylogenetic structure. Ecography (Cop). 40 (8):913–929. doi: 10.1111/ecog.02881.

Sabato EO, Landau EC, Barros BA, Oliveira CM. 2020. Differential transmission of *phytoplasma* and *spiroplasma* to maize caused by variation in the environmental temperature in Brazil. null. 157(1):163–171. doi: 10.1007/s10658-020-01997-9.

Santana PA, Kumar L, Da Silva RS, Pereira JL, Picanco MC. 2019. Assessing the impact of climate change on the worldwide distribution of *Dalbulus maidis*. (delong) Using maxent Pest Manag Sci. 75 (10):2706–2715. doi: 10.1002/ps.5379.

Santini L, Benítez-López A, Maiorano L, Čengić M, Huijbregts MAJ. 2021. Assessing the reliability of species distribution projections in climate change research. Divers Distrib. 27 (6):1035–1050. doi: 10.1111/ddi.13252.

Saupe EE, Barve V, Myers CE, Soberón J, Barve N, Hensz CM, Peterson AT, Owens HL, Lira-Noriega A. 2012. Variation in niche and distribution model performance: the need for a priori assessment of key causal factors. Ecol Modell. 237–238:11–22. doi: 10.1016/j.ecolmodel.2012.04.001.

Schartel TE, Cao Y. 2024. Background selection complexity influences Maxent predictive performance in freshwater systems. Ecol Modell. 488 (December 2023):110592. doi: 10.1016/j.ecolmodel.2023.110592.

Sillero N. 2011. What does ecological modelling model? A proposed classification of ecological niche models based on their underlying methods. Ecol Modell. 222(8):1343–1346. doi: 10.1016/j.ecolmodel.2011.01.018.

Sillero N, Barbosa AM. 2021. Common mistakes in ecological niche models. Int J Geogr Inf Sci. 35(2):213–226. doi: 10.1080/13658816.2020.1798968.

Singh BK, Delgado-Baquerizo M, Egidi E, Guirado E, Leach JE, Liu H, Trivedi P. 2023. Climate change impacts on plant pathogens, food security and paths forward. Nat Rev Microbiol. 21(10):640–656. doi: 10.1038/s41579-023-00900-7.

Soberon JM. 2010. Niche and area of distribution modeling: a population ecology perspective. Ecography (Cop). 33(1):159–167. doi: 10.1111/j.1600-0587.2009.06074.x.

Soberon JM, Peterson AT. 2005. Interpretation of models of fundamental ecological niches and species' distributional areas. Biodivers Inf. 2 (10):3392–3396. doi: 10.17161/bi.v2i0.4.

Tonle FBN, Niassy S, Ndadji MMZ, Tchendji MT, Nzeukou A, Mudereri BT, Senagi K, Tonnang HEZ. 2024. A road map for developing novel decision support system (DSS) for disseminating integrated pest management (IPM) technologies. Comput Electron Agric. 217(May 2023):108526. doi: 10.1016/j.compag.2023.108526.

Valavi R, Elith J, Lahoz-Monfort JJ, Guillera-Arroita G, Warton D. 2019. BlockCV: an r package for generating spatially or environmentally separated folds for k-fold cross-validation of species distribution models. Methods Ecol Evol. 10(2):225–232. doi: 10.1111/2041-210X.13107.

Van Nieuwenhove GA, Frías EA, Virla EG. 2016. Effects of temperature on the development, performance and fitness of the corn leafhopper *Dalbulus maidis* (DeLong)(H emiptera: C icadellidae): implications on its distribution under climate change. Agric For Entomol. 18(1):1–10. doi: 10.1111/afe.12118.

VanDerwal J, Shoo LP, Johnson CN, Williams SE. 2009. Abundance and the environmental niche: environmental suitability estimated from niche models predicts the upper limit of local abundance. Am Nat. 174 (2):282–291. doi: 10.1086/600087.

Varela S, Anderson RP, García-Valdés R, Fernández-González F. 2014. Environmental filters reduce the effects of sampling bias and improve predictions of ecological niche models. Ecography (Cop). 37 (11):1084–1091. doi: 10.1111/j.1600-0587.2013.00441.x.

Velazco SJE, Rose MB, de Andrade AFA, Minoli I, Franklin J. 2022. Flexsdm: an r package for supporting a comprehensive and flexible species distribution modelling workflow. Methods Ecol Evol. 13 (8):1661–1669. doi: 10.1111/2041-210X.13874.

Velazco SJE, Villalobos F, Galvão F, De Marco Júnior P, Serra-Diaz J. 2019. A dark scenario for cerrado plant species: effects of future climate, land use and protected areas ineffectiveness. Divers Distrib. 25 (4):660–673. doi: 10.1111/ddi.12886.

Vignali S, Barras AG, Arlettaz R, Braunisch V. 2020. Sdmtune: an R package to tune and evaluate species distribution models. Ecol Evol. 10(20):11488–11506. doi: 10.1002/ece3.6786.

Virla EG, Coll Araoz MV, Luft Albarracin E. 2021. Estimation of direct damage to maize seedlings by the corn leafhopper, *dalbulus maidis* (Hemiptera: Cicadellidae), under different watering regimes. Bull Entomol Res. 111(4):438–444. doi: 10.1017/S0007485321000079.

Von Storch JS, Haak H, Hertwig E, Fast I, von Storch J-S. 2016. Vertical heat and salt fluxes due to resolved and parameterized meso-scale eddies. Ocean Model. 108:1–19. doi: 10.1016/j.ocemod.2016.10.001.

Wang Z, Xu D, Liao W, Xu Y, Zhuo Z. 2023. Predicting the current and future distributions of *Frankliniella occidentalis* (Pergande) based on the MaxEnt species distribution model. Insects. 14(5):1–12. doi: 10.3390/insects14050458.

Waquil JM, Viana PA, Cruz I, Jamilton E, Santos P. 1999. Aspectos da biologia da cigarrinha-do-milho, *Dalbulus maidis* (DeLong & Wolcott) (Hemiptera: Cicadellidae) (DeLong and Wolcott) (Hemiptera: Cicadellidae). MG An Soc Entomol Bras. 28(3):413–420. doi: 10.1590/S0301-80591999000300005.

Wheeler T, von Braun J. 2013. Climate change impacts on global food security. Science. 341(6145):508–513. doi: 10.1126/science.1239402.

Wickham H. 2018. Scales: scale functions for visualization. [accessed 2023 Jan 23]. https://cran.r-project.org/package=scales.

Yukimoto S, Kawai H, Koshiro T, Oshima N, Yoshida K, Urakawa S, Tsujino H, Deushi M, Tanaka T, Hosaka M, et al. 2019. The meteorological research institute Earth system model version 2.0, MRI-ESM2.0: description and basic evaluation of the physical component. J Meteorol Soc Jpn. 97(5):931–965. doi: 10.2151/jmsj.2019-051.